

Annual Review of Condensed Matter Physics
Organization and
Self-Assembly Away from

Equilibrium: Toward
Thermodynamic Design

Principles

Michael Nguyen, Yuqing Qiu, and Suriyanarayanan Vaikuntanathan

Department of Chemistry and The James Franck Institute, University of Chicago, Chicago, Illinois 60637, USA; email: svaikunt@uchicago.edu

Annu. Rev. Condens. Matter Phys. 2021. 12:273-90

The Annual Review of Condensed Matter Physics is online at commatphys.annualreviews.org

https://doi.org/10.1146/annurev-conmatphys-031218-013309

Copyright © 2021 by Annual Reviews. All rights reserved

ANNUAL CONNECT

www.annualreviews.ora

- · Download figures
- Navigate cited references
- Keyword search
- · Explore related articles
- · Share via email or social media

Keywords

self-assembly, stochastic thermodynamics, second law of thermodynamics, active matter, soft matter, fluctuation and noise, irreversible process

Abstract

Studies of biological systems and materials, together with recent experimental and theoretical advances in colloidal and nanoscale materials, have shown how nonequilibrium forcing can be used to modulate organization in many novel ways. In this review, we focus on how an accounting of energy dissipation, using the tools of stochastic thermodynamics, can constrain and provide intuition for the correlations and configurations that emerge in a nonequilibrium process. We anticipate that the frameworks reviewed here can provide a starting point to address some of the unique phenomenology seen in biophysical systems and potentially replicate them in synthetic materials.

1. INTRODUCTION

Biological systems and materials use nonequilibrium forces to modulate self-assembly and organization in a variety of novel ways (1–12). Kinetic proofreading mechanisms (13, 14) show how errors in various replication and information processing tasks in biology (15) can be reduced at the cost of energy consumption. *Escherichia coli* flagellar motors (11, 12, 16) exhibit unique phenomenology such as ultrasensitive response, adaptation (10), and motor restructuring as a function of applied torque (11). These important functional features are powered by nonequilibrium driving (10, 12, 17). On larger scales, biopolymers such as actin and microtubules are used to perform a variety of tasks, from force sensing (18, 19) to segregation of biological material (20–22). Many of these features are powered by nonequilibrium forcing due to molecular motor activity (23–25). On the whole, this rich phenomenology points to the need to develop an understanding of how nonequilibrium forces drive such organization. Such an understanding would in turn enable identification of design principles for (bioinspired) synthetic soft matter systems that can sense, process, adapt, and respond to stimuli at the cost of energy consumption (21, 26, 27).

Recent works have also identified new and specific ways in which nonequilibrium forces can be used to achieve novel organization and functionality in synthetic many-body nonequilibrium systems (1, 4, 5, 7, 28–41). Examples include assemblies driven by light (28–32) and by magnetic fields and electric fields (35, 36), supramolecular assemblies (37–39), and nonequilibrium pattern formation (40, 41). These and other studies of active and driven matter systems have revealed how energy consumption on the microscale can be parlayed into rules for mesoscale self-assembly and organization (42–48). In many of these examples, it has been demonstrated that by controlling the driving forces, one can imbue to the system many properties that are impossible or improbable to have at equilibrium. For example, in Reference 36, by controlling the frequency of an electric field, a system composed of metal dielectric Janus colloids can be programmed to dynamically assemble into chains, clusters, or swarms.

In this review, we focus on thermodynamic frameworks that can elucidate the tradeoffs among energy consumption, speed of assembly, and organization as soft materials are assembled or grown in nonequilibrium conditions (49, 50). In particular, we focus on how ideas from stochastic thermodynamics (51–54) can be used to first quantify metrics of dissipation or entropy production and then use such metrics to guide self-assembly and organization in complex many-body nonequilibrium systems.

First, in Section 2, we specifically consider the self-assembly and growth of nonterminal structures such as crystals, fibers (42, 55, 56), and membranes (43) under nonequilibrium conditions. We review how ideas from stochastic thermodynamics, such as the newly discovered thermodynamic uncertainty relations (57, 58), can be used to constrain changes in compositions (42) and morphology (43) due to nonequilibrium driving. In Section 3, we consider self-assembly and organization in active or driven media (44, 46). Unlike Section 2, the nonequilibrium forcing here is not coupled to growth. We review how an application of stochastic thermodynamics and ideas developed in the context of large deviation theories (59) can be used to elucidate the tradeoffs between energy consumption and organization in such systems. Finally, for each of the frameworks reviewed, we conclude with a list of future challenges and opportunities.

Understanding and controlling self-assembly and organization in nonequilibrium conditions have been proposed as one of the most important problems in statistical mechanics (27). This review has a very specific and narrow focus: namely, elucidating the extent to which the energy dissipation rates can be used to predict or constrain the outcome of nonequilibrium organization processes. As such, the current review does not cover many of the other prerequisites required to explain some of the above described novel phenomenology observed in nonequilibrium biological and synthetic systems. Nonetheless, we hope that this work clarifies some of the

thermodynamic constraints required to stabilize desired configurations or structures at the cost of energy dissipation.

2. NONEQUILIBRIUM GROWTH PROCESS

The fields of colloidal and nanoscale self-assembly have seen dramatic progress in the past few years (60–68). However, most of these advances are based on an equilibrium thermodynamic framework: The target configuration minimizes a thermodynamic free energy (69). Understanding the principles governing self-assembly and organization in far-from-equilibrium systems remains one of the central challenges of nonequilibrium statistical mechanics (21, 27). Indeed, even with the recent advances in nonequilibrium statistical mechanics, such as the discovery of fluctuation theorems (70), no universal framework for the control of steady states in such growing many-body systems has been developed. Classical ideas based on Onsager's regression relation and linear irreversible thermodynamics have previously been used to obtain equations to describe nonequilibrium phenomena in soft matter (71). However, these are valid close to equilibrium and are not immediately extendable to nonequilibrium growth processes.

To be more precise, imagine a self-assembly process in which a structure is assembled by assimilating monomers from a bath. Assume that the interactions among the various particles in the system are described by a set of energies E_{eq}. Typically, such energies can be readily derived from an atomistic force field. We imagine that the growth rate of the system can be varied by tuning the concentration of monomers in the bath or equivalently the chemical potential of the bath. We use $\mu_{\rm coex}$ to denote the value of the chemical potential for which the system does not grow on average (and is in equilibrium). The system can be made to grow at a finite rate by tuning the chemical potential to a value above this coexistence value. The excess chemical potential $\delta \mu \equiv \mu - \mu_{\rm coex}$ is the nonequilibrium driving force in this setup. This generic setup is sufficient to describe many self-assembly processes (42). At equilibrium, $\delta \mu = 0$, and the configuration of the system and/or assembly can be predicted by computing the equilibrium partition function and free energy $G_{\rm eq}$ appropriate to the set of interaction energies. Away from equilibrium, the free-energy landscape does not predict the configurations sampled. In general, for such a prediction, detailed kinetic information describing the nonequilibrium growth process is required (72-74). However, as we discuss below, an accounting of the entropy production rate along with an application of recently discovered identities such as the thermodynamic uncertainty relations might make it possible to substantially constrain the allowed configurations observed in a nonequilibrium growth process even with minimal kinetic information.

2.1. Entropy Production

We begin by writing down the second law of thermodynamics for such growth processes (52, 75, 76). The phenomenological derivation provided below is most closely related to that discussed in References 77 and 78 and has been used in other contexts such as in References 42, 79, and 80. Indeed, expressions for the entropy production rate in nonequilibrium polymerization processes are already provided in the pioneering work in References 77 and 78. The results reviewed below adapt these expressions so that they can be used to constrain the configurations observed in nonequilibrium self-assembly processes. Let $P_t(\omega, N)$ denote the probability distribution associated with observing a system size of N and a microscopic configuration ω at a particular instant of time. The entropy of the system, S, is given by the configuration

$$S = -k_{\rm B} \sum_{\omega, N} P_t(\omega, N) \ln P_t(\omega, N),$$
 1.

where $k_{\rm B}$ is the Boltzmann constant. To proceed, following Reference 77, we decompose the distribution $P_t(\omega,N)$ as $P_t(\omega,N) \equiv P_t(N)p_N(\omega)$, where $P_t(N)$ and $p_N(\omega)$ are both normalized probability distributions. In performing the decomposition, we have assumed that the system has reached a steady state and that distribution of compositional fluctuations for a given system size, $p_N(\omega)$, is independent of the time t. With this assumption, we associate with the distribution, $p_N(\omega)$, an effective energy functional, $E_{\rm eff}(\omega)$, and an effective free energy, $F_{\rm eff}$, such that $E_{\rm eff}(\omega) - F_{\rm eff} = -k_{\rm B}T\ln p_N(\omega)$. This is simply a statistical defining relation for the energy function (analogous to a potential of mean force). The energy function $E_{\rm eff}(\omega)$ does not control the dynamics of the system. This effective energy function can have a form very different from that of the interactions specified by the interaction Hamiltonian, $E_{\rm eq}(\omega)$. Assuming that the functional form of $E_{\rm eff}$ is independent of N, and using the relation $E_{\rm eff}(\omega) - F_{\rm eff} = -k_{\rm B}T\ln p_N(\omega)$, the entropy of the growing system in Equation 1 can be rewritten as

$$TS = \langle N \rangle_t \frac{-F_{\text{eff}} + \langle E_{\text{eff}} \rangle_N}{N}.$$
 2.

Here, $\langle ... \rangle_N$ is the average of all microscopic configurations of the assembly with respect to the distribution, $p_N(\omega)$, at size $N \gg 1$, and $\langle N \rangle_t$ is the average size of the assembly after it has been allowed to grow for a time t. In addition, when the bath size is much bigger than the assembly, the entropy exchanged between the bath and the growing assembly is

$$T\Delta S_{\text{bath}} = -\langle N \rangle_t \frac{-F_{\text{eq}} + \langle E_{\text{eq}} \rangle_N - N\delta\mu}{N}.$$
 3.

Combining the two entropies in Equations 2 and 3, we can write down the total entropy of the process, which must be nonnegative according to the second law of thermodynamics (42):

$$T \frac{\mathrm{d}S_{\mathrm{total}}}{\mathrm{d}t} \approx \frac{\mathrm{d}\langle N \rangle}{\mathrm{d}t} \left(\delta \mu - \langle \epsilon_{\mathrm{diss}} \rangle \right) \ge 0.$$
 4.

Here, $\langle \epsilon_{\rm diss} \rangle = [\langle E_{\rm eq} - E_{\rm eff} \rangle_N - (F_{\rm eq} - F_{\rm eff})]/N$. For growing assemblies, $\frac{{\rm d}\langle N \rangle}{{\rm d}t} \geq 0$, and the constraint in Equation 4 reduces to $\delta \mu \geq \langle \epsilon_{\rm diss} \rangle$. The term $\langle \epsilon_{\rm diss} \rangle$ can be viewed as a thermodynamic reorganization cost for creating structures that are different from those corresponding to the equilibrium landscape, $E_{\rm eq}$. Because Equation 4 is a statement of the second law of thermodynamics, it is effectively independent of the kinetics of the nonequilibrium growth process. We note again that similar equivalent statements of the second law of thermodynamics have been written down in the context of a variety of polymerization processes (77–80).

2.2. Thermodynamic Uncertainty Relations

Close to equilibrium, Onsager's fluctuation dissipation relation provides a hint that constraints such as those in Equation 4 might be further refined. Specifically, interpreting $\delta\mu - \langle \epsilon_{\rm diss} \rangle$ as an effective force driving the increase in the assembly size, the fluctuation dissipation relation implies that the response, $v \equiv \langle \dot{N} \rangle$, is proportional to the driving force with the proportionality constant being related to the fluctuations in the growth rate, $D = \lim_{\tau \to \infty} \frac{\langle \Delta N^2 \rangle}{2\tau}$ (71, 81). Such arguments form the basis of the framework of linear irreversible thermodynamics and have been used successfully to describe the dynamics of active gels, biological membranes, and liquid membranes.

A newly discovered class of relations in stochastic thermodynamics, the thermodynamic uncertainty relations (57, 58), suggests that such fluctuation dissipation relations can be extended to far-from-equilibrium conditions. Specifically, these relations suggest that the entropy production rates generically bound the relative fluctuations of all fluxes in the system. In their most generic

form, these relations can be written as

$$\Sigma \ge \frac{2k_{\rm B}\langle J_{\alpha}\rangle^2}{Var(J_{\alpha})}.$$

Here, Σ is the total entropy production of the process. J_{α} is a generalized current that, in principle, can be a linear combination of fluxes; $\langle J_{\alpha} \rangle$ is the average generalized current; and $Var(J_{\alpha})$ is its variance. The thermodynamic uncertainty relations were first derived using large deviation theory to analyze the statistics of current fluctuations in Markov state networks (58). Close to equilibrium, the thermodynamic uncertainty relations are equivalent to statements of the fluctuation dissipation relation or linear response theory. These relations have been extensively reviewed elsewhere (57, 58). By extending these relations to finite-time nonequilibrium processes, time-dependent nonequilibrium processes have also been explored (82–85). Finally, similar classes of relations can also be derived for other statistical quantities such as first passage times (86).

If the thermodynamic uncertainty relations can be extended to the problem of nonequilibrium self-assembly, they result in an inequality of the form

$$\delta\mu - \langle \epsilon_{\rm diss} \rangle \ge \frac{v}{D}$$
,

where, in the context of self-assembly, we are interested in the generalized flux $J_{\alpha} \equiv v \equiv \frac{\mathrm{d}\langle N \rangle}{\mathrm{d}t}$. Given a nonequilibrium driving force $\delta \mu$ and equilibrium interactions E_{eq} , the statistics of growth rates, v or $\frac{\mathrm{d}\langle N \rangle}{\mathrm{d}t}$, is the average rate of growth of the assembly, and D is related to the variance of growth rate fluctuations of the assembly. Equation 6 provides a variational principle for estimating E_{eff} , the effective energy functional that describes the correlations in the nonequilibrium assembly. This equation has the potential to elucidate tradeoffs among energy consumption, speed, and organization for nonequilibrium self-assembly. Specifically, given a nonequilibrium driving force, $\delta \mu$, and the ratio v/D, Equation 6 provides a bound on the reorganization energy cost, $\langle \epsilon_{\mathrm{diss}} \rangle$, that is available in the nonequilibrium growth process. Thus, Equation 6 provides a bound on the configurations that can be accessed in a nonequilibrium growth process (which we discuss in more detail below). The reorganization cost, $\langle \epsilon_{\mathrm{diss}} \rangle$, can also be expressed as an information theoretic cost, $\langle \epsilon_{\mathrm{diss}} \rangle \equiv D[\rho || \rho_{\mathrm{eq}}]/N$, where $D[\rho || \rho_{\mathrm{eq}}]$ is the relative entropy between the observed steady-state distribution of configurations ρ in the nonequilibrium assembly of size N and the distribution of configurations ρ_{eq} of the assembly grown close to equilibrium, i.e., $\delta \mu \sim 0$.

Before proceeding to review specific applications of Equation 6, we note that the thermodynamic uncertainty relations (57, 58) have formally been derived for Markov processes on finite graphs, whereas a growing assembly has no finite size constraints. Thus, the application of such thermodynamic uncertainty relations to self-assembly problems needs to be done with care. In Reference 42, we showed how such an extension can be achieved by mapping the dynamics of a one-dimensional self-assembly process onto the dynamics of a time-independent finite-state Markov process. In general, we anticipate that as long as the correlations in the growing assembly are bounded and can be described by time-independent energy functions $E_{\rm eff}$, the dynamics of the nonequilibrium self-assembly process can be mapped on the dynamics of a complex but finite Markov state network. The thermodynamic uncertainty relations can hence be applied to the finite Markov state caricature. Therefore, Equations 4 and 6 may be used to predict or bound the correlations generated in the course of nonequilibrium self-assembly (42).

2.3. Predicting Compositions and Phase-Transition Behavior

To illustrate the effectiveness of Equation 6, we considered one- and two-dimensional lattice-based assembly problems introduced first in References 55 and 56. The model contains two

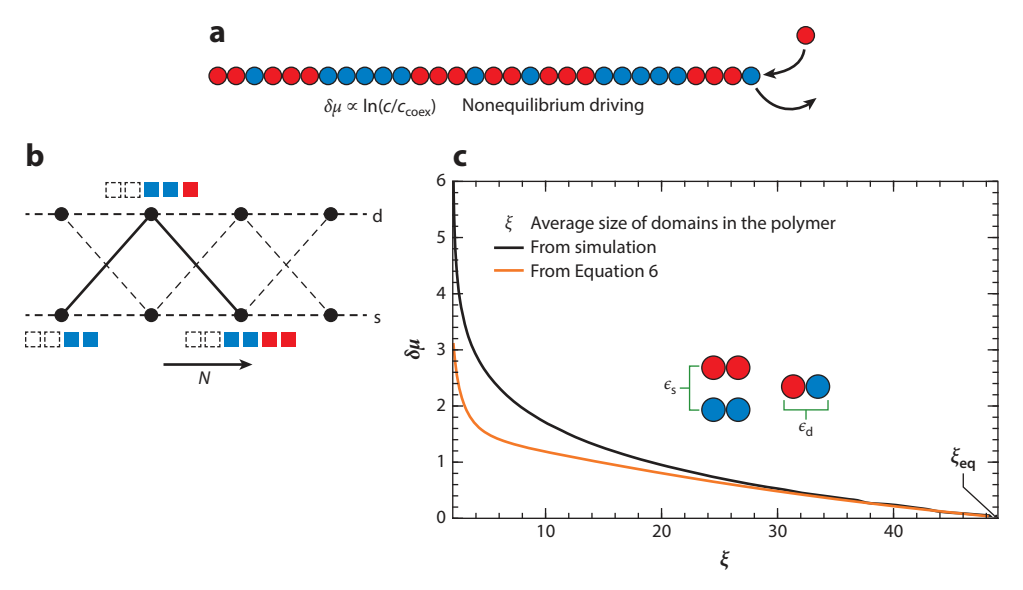


Figure 1

Domain lengths bound using Equation 6 in a nonequilibrium growth process. (a) Schematic of the 1D assembly growth process. The assembly consists of two types of monomers (red and blue). (b) Schematic of the effective Markov state model. The Markov state model resolves the nature of the terminal bond in the self-assembled system (vertical rungs) and the number of particles in the self-assembled system (N; borizontal axes). The s stands for a bond between similar or like monomers and the d stands for a bond between different or unlike monomers. (c) Comparison between the lower bounds of $\delta\mu$ obtained using Equation 6 (orange curve) and from simulation (black curve). Figure adapted from Reference 42.

types of monomers (with equal concentrations in the bath) and is grown from one end. Only nearest-neighbor interactions between monomers in the system are allowed, with ϵ_s denoting the energy of interaction between identical monomers and ϵ_d denoting the energy of interaction between unlike monomers. When $\delta \mu = 0$, the system is at equilibrium, and its compositional fluctuations resemble those of an Ising model with a coupling constant $J = (\epsilon_s - \epsilon_d)/2$. When grown out of equilibrium, Equation 6 can be used to look for the effective nearest-neighbor coupling constant, Jeff, that most accurately describes the compositions in the growing assembly. In the case of one-dimensional assemblies (Figure 1), Equation 6 was able to predict or bound the compositional fluctuations very accurately even far from equilibrium (42). The twodimensional assembly (Figure 2) exhibits more complex phenomenology. By tuning the nonequilibrium forcing, $\delta \mu$, the system can be made to exhibit compositional fluctuations resembling those seen at the critical point of a two-dimensional Ising model (56) (even though the physical interaction strengths, ϵ_s and ϵ_d , remain unmodified). In other words, nonequilibrium forcing seems to drive the system toward a second-order phase transition (56). As a first approximation, we used Equation 6 to obtain estimates of effective nearest-neighbor coupling strengths Jeff that can most accurately describe the compositional fluctuations in the growing system. The values of $J_{\rm eff}$ obtained from Equation 6 provide reasonably tight bounds on the compositional fluctuations observed in the growing assembly and even provide a reasonably accurate bound for the value of the driving force $\delta\mu_c$ at which critical compositional fluctuations are accessed (42) (Figure 2).

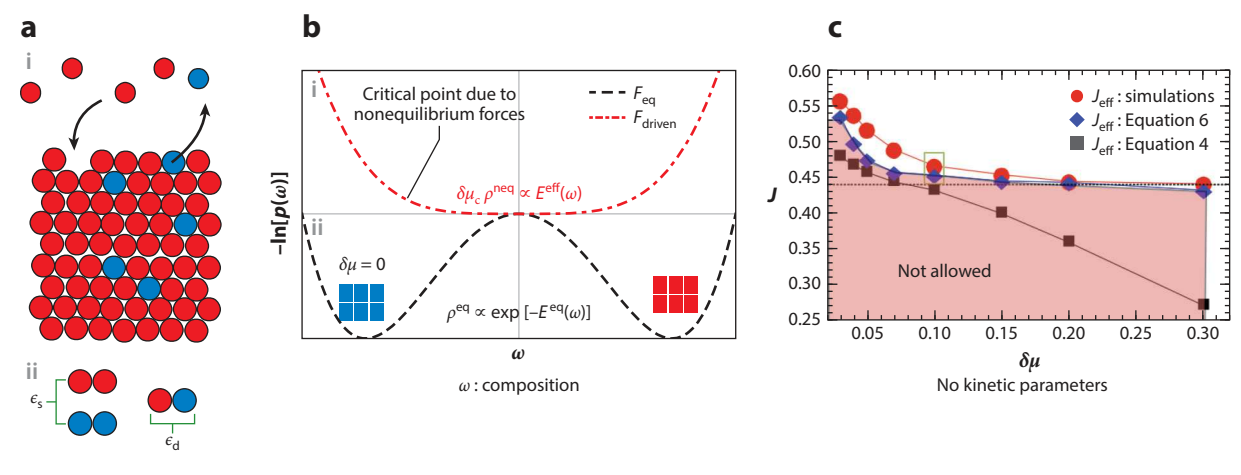


Figure 2

Prediction of nonequilibrium phase transition behavior using Equation 6. (a) Equation 6 was applied to a model lattice-based self-assembly problem in which a two-dimensional binary assembly is grown (56). ϵ_s denotes the energy of interaction between identical components and ϵ_d denotes the energy of interaction between unlike components. (b) When the assembly is grown at equilibrium, the statistics of compositional fluctuations in the assembly are equivalent to that of an Ising magnet with coupling constant $J = \frac{\epsilon_s - \epsilon_d}{2}$. Recent work in Reference 56 showed that such nonequilibrium driving can drive the compositional fluctuations in the system to a second-order phase transition. Equation 6 is able to bound such changes in the effective free-energy landscape. For instance, the graph in panel ϵ compares the effective magnetic constant, ϵ 0, from the simulations with those predicted from Equations 4 and 6. This demonstrates that Equation 6 can place accurate bounds on the compositional fluctuations excited during the nonequilibrium growth process and also provide an accurate bound on the location of the driving force, ϵ 1, required to excite the critical fluctuations. Figure adapted from Reference 42.

2.4. Morphological Changes in Model Membranes Due to Nonequilibrium Driving

The nonequilibrium variational theorem may also be applied to understand how material properties of membranes (biophysical and synthetic), such as the surface tension, can be modulated using nonequilibrium forcing (**Figure 3**). The role played by nonequilibrium forces in biological processes such as those responsible for modulating cell shapes and dynamics is well established (87–91). Indeed, experiments on model lipid vesicles that can absorb lipids from a surrounding bath and grow have shown that nonequilibrium driving can force morphological transitions after which the vesicles no longer grow with a spherical shape (92–94)—such systems and transitions can potentially be good models for studying the thermodynamics of endocytosis (93) and cell shape changes (92, 94). Recent work in Reference 73 used hydrodynamic simulations to show how various morphologies that are functionally relevant for endocytosis and cell division can be accessed when a membrane is forced to grow. A nonequilibrium theory for the control of material properties and morphology in such systems can hence be very useful as it can elucidate tradeoffs between energy consumption and organization.

The nonequilibrium variational theorem in Equation 6 can potentially be used to probe the tradeoffs between energy consumption and organization in such a nonequilibrium growth process. Preliminary results along these lines have been obtained in Reference 43 in which the growth of a model one-dimensional elastic string (embedded in two dimensions; see **Figure 3***b*) was studied. As in the previous preliminary results, the chemical potential of the reservoir controls the growth rate of the ring assembly and sets the nonequilibrium driving force in this system. In particular, beyond a critical value of $\delta \mu > \delta \mu_c$, the assembly no longer grows in a circular shape (**Figure 3***b*,*c*).

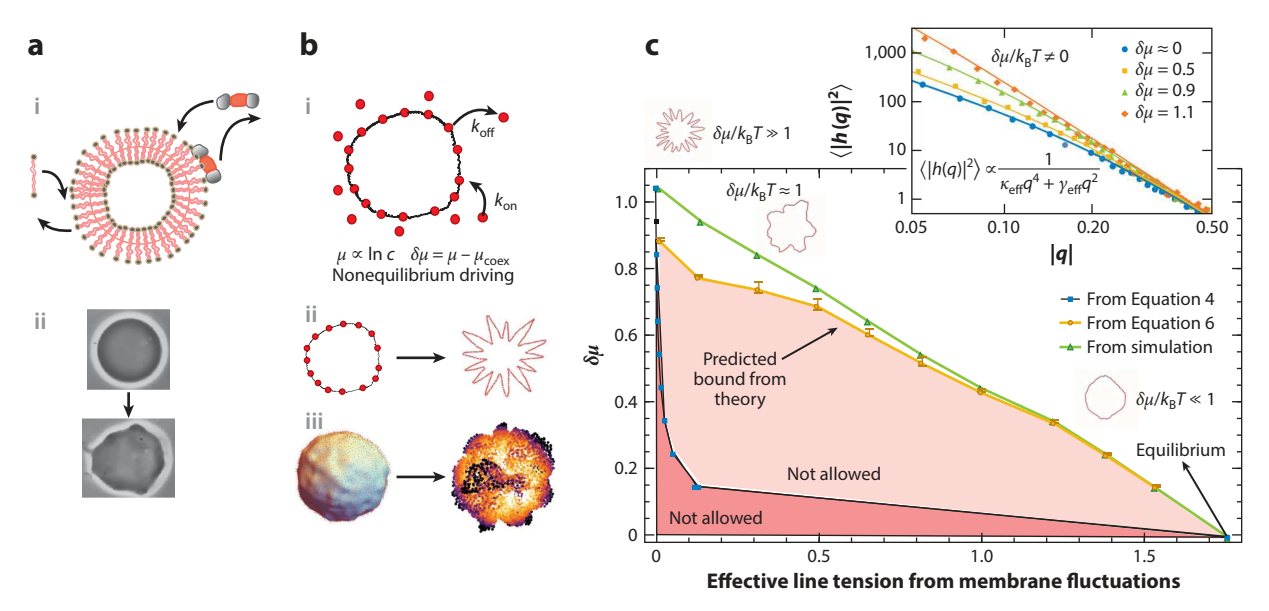


Figure 3

(a) The nonequilibrium variational theory is used to study growth-induced morphological transitions in biophysical and synthetic membranes. (a, i) Biological membranes undergo constant remodeling due to either growth or binding—unbinding of variance membrane proteins. (a, ii) Experimental observations of morphological changes in vesicles due to the growth. (b, i) Growth and morphological transitions studied in a model elastic string. (b, ii) Morphological changes in string geometry can be accessed by forcing the system to grow beyond a critical rate. (b, iii) Similar morphological transitions can be observed when two-dimensional membrane surfaces are forced out of equilibrium. (c) As $\delta\mu$ is increased, the effective line tension—like parameter, γ_{eff} , of the string decreases, eventually reaching $\gamma_{\text{eff}} \approx 0$ for $\delta\mu \approx 1.1$. Increasing $\delta\mu$ beyond this value induces a morphological change to a configuration with spikes. The green curve represents the effective line tensions measured in simulations. The nonequilibrium variational theory in Equation 6 (*orange curve*) provides a more accurate bound for the renormalization of the line tension due to nonequilibrium forcing in comparison to the bound given by Equation 4 (*black curve*). (*Inset*) The values of γ_{eff} from simulations were obtained by computing the power spectrum of radial fluctuations and fitting the spectrum to expectations from Helfrich elasticity theory (43). The values of the elastic constants estimated in this way were independent of the size of the assembly in agreement with our theoretical expectations. Panel a adapted from Reference 92 with permission.

We analyzed the spectrum of string fluctuations in the nonequilibrium simulations and, assuming an effective Helfrich-like form, extracted effective line tension–like (γ_{eff}) and bending rigidity–like parameters. We found that the nonequilibrium driving renormalizes the value of the effective line tension–like parameter obtained in this way. In particular, close to the morphological transition, the effective line tension parameter is renormalized to zero. We stress that this effective line tension–like parameter is simply a convenient way to characterize the fluctuations in the nonequilibrium system.

The nonequilibrium variational theorem, Equation 6, can be used to obtain estimates of the effective line tension, $\gamma_{\rm eff}$, as a function of $\delta\mu$. In particular, the reorganization cost, $\langle\epsilon_{\rm diss}\rangle$, in Equation 6 can be used to search for effective line tension–like values, $\gamma_{\rm eff}$, that describe the fluctuations in the configurations of the growing membrane. The results in **Figure 3***c* suggest that the theory is able to bound and predict the renormalization of such effective line tension observed in simulations without any kinetic details of the assembly process (beyond v/D).

In summary, accounting for the entropy production rates in nonequilibrium growth and self-assembly problems, through the formalism of stochastic thermodynamics, can potentially reveal or constrain the configurations and correlations that are formed due to the nonequilibrium forcing.

In particular, Equation 6 provides a bound on $\langle \epsilon_{\text{diss}} \rangle$, which is a measure of the dissipated energy cost to restructure the assembly from the energy landscape, E_{eq} to E_{eff} .

3. ORGANIZATION IN DRIVEN AND ACTIVE MEDIA

Model-driven and active-matter systems (8, 95-97) have provided an analytically and computationally tractable test bed to study organization in nonequilibrium systems. Models of driven systems can be realized experimentally in a variety of ways, for instance, using external electric and magnetic fields (27, 98-100), and lead to a variety of rich phenomenology including phase transitions (44, 98), large mesoscopic currents along interfaces (5), and dynamic assembly into moving nanocrystals and tubes (100). Activity can also be used to promote various novel reorganization pathways and increase the yield of novel structures, as was demonstrated in Reference 101, where active Janus-like particles were used to enhance the self-assembly yield of Kagome lattices. Inspired by phenomenology exhibited by actin and microtubule assemblies, studies of active nematic materials have shown how nematic elastic constants and morphology can be modulated by nonequilibrium driving (102). It has also been demonstrated that nonequilibrium chiral activity can be used to create materials with novel elastic and transport properties that are unattainable at equilibrium. Attempts at constructing a unified theoretical framework in such systems have used effective temperature-like caricatures (98), developed prescriptions to compute pressure and stresses in nonequilibrium media (103, 104) and developed effective thermodynamic frameworks to explain various phase-transition and coexistence phenomena (105).

Interestingly, and of particular relevance to this article, recent work has also suggested that accounting for (46, 106–108) and controlling the various rates of dissipation in active and driven media might provide a convenient way to control and anticipate the properties of some of the above described nonequilibrium media. Below, we review these ideas.

3.1. Controlling Structure Using Biased Energy Flows

In order to introduce the framework, we begin by considering a model-driven liquid composed of two particle types (**Figure 4***a*). All particles of type A are driven in phase by an external field. Both particle types are modeled as point particles with no additional degrees of freedom. Such a system was first introduced in Reference 98 to model colloidal particles driven differently by external magnetic fields. The external forces do work on the system by driving particles of type A into type B. This energy flow has been shown to induce phase separation in this system (44, 98).

In order to investigate how such energy fluxes affect the microscopic interactions in very general settings, imagine turning off the external driving and simply consider biasing the dynamics in terms of the rate of potential energy stored in the A–B interactions. Specifically, instead of channeling energy into the system by inducing collisions between A and B particles (as the external driving would have done), the framework of large deviation theory and biased sampling techniques (109–112) are used to harvest trajectories that either pump energy into or extract energy from the A–B interactions at a finite rate. Such biased sampling can be achieved using techniques developed to compute large deviation functions of various quantities. Specifically, given a physical trajectory-dependent observable $\varepsilon(t)$, biasing can be achieved by formally introducing an exponential weighting function $\exp [k \cdot \varepsilon(t)]$ in the path probability of the microscopic dynamics as defined within the framework of large deviations (113, 114). Here, the variable ε is extensive in time, and its average rate $\varepsilon(t)/t$ in the biased ensemble is controlled by the bias amplitude k at large time $t \to \infty$. Therefore, the biased ensemble enables one to probe system configurations associated with different rates $\varepsilon(t)/t$, simply by modulating the external parameter k.

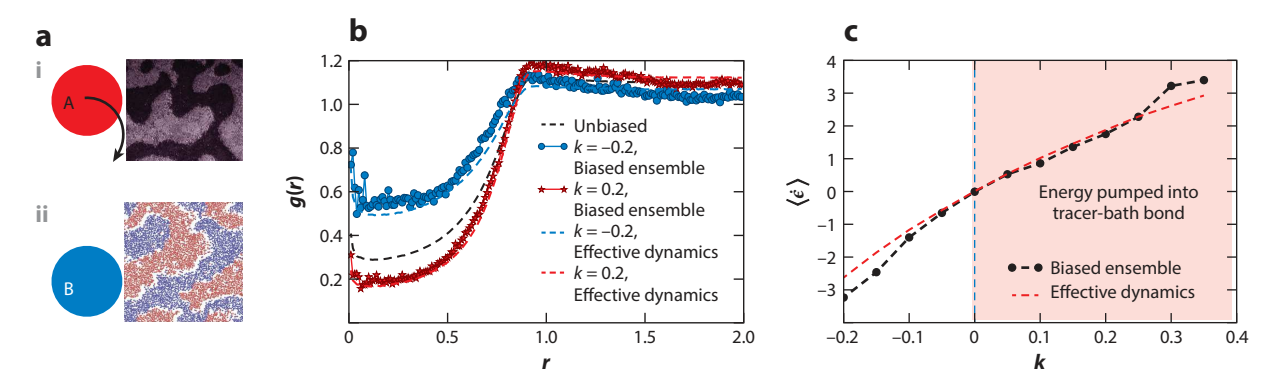


Figure 4

(a) Model of a two-component liquid with one component driven by an external field. An experimental system, designated as A (subpanel i), with similar dynamics undergoes phase separation. Phase separation, designated as B (subpanel ii), is shown in simulations of the model liquid due to driving. Subpanel i adapted with permission from Reference 98, and subpanel ii adapted with permission from Reference 44. (b) Plot of the A–B pair correlation function for various energy-biasing strengths k compared with analytical predictions from Equation 8. (c) Plot of $\langle \dot{\epsilon} \rangle$ as a function of the biasing field k obtained from both simulations of the biased ensemble using the cloning algorithm and equilibrium simulations with Equation 8. Together, these results show how energy biasing can modify the structure of the fluid. For values of k > 0 when energy is pumped into the tracer-bath interactions, the tracer and bath particles effectively repel each other more strongly, in agreement with Equation 8. Such enhanced repulsion can potentially favor phase separation of the sort seen in panel a.

For particles evolving according to overdamped Langevin equations of motion with a friction constant γ and a random Gaussian forcing $\eta(t)$ with $\langle \eta(t)\eta(t')\rangle = 2T\delta(t-t')$, a specific functional form for $\varepsilon(t)$ can be obtained within the Ito convention (115),

$$\varepsilon(t) = \frac{1}{\gamma} \int_0^t \left[T \nabla_i^2 V_{A-B} + (\nabla_i V_{A-B}) \cdot (\mathbf{F}_i) \right] ds,$$
 7.

where \mathbf{F}_i is the conservative force acting on particle i and $V_{\mathrm{A-B}}$ is the potential energy stored in the A–B interactions. $\mathrm{d}\varepsilon/\mathrm{d}t$ is indeed equal to the rate of change of $V_{\mathrm{A-B}}$ averaged over all realizations of the random noise $\eta(t)$ for the above described overdamped Langevin equation of motion (46). In the unbiased case k=0, the energy flow vanishes due to the fluctuation dissipation relation (44).

By tuning k positive or negative, trajectories that preferentially cause energy flow into or extract energy from the system can be generated. Hence, sampling this ensemble of trajectories provides an indirect, if somewhat contrived, way to assess how energy flows can modify the properties of interacting many-body systems. Such trajectory biases have been used in other contexts to explore, for example, dynamical heterogeneities in glassy systems (109–111, 116–119), soliton solutions in high-dimensional chaotic chains (120, 121), and the clustering of active self-propelled particles (106, 122). In practice, the configurational steady state obtained by such trajectory biasing tends to be highly nontrivial for many-body systems (113). However, for the energy biasing in Equation 7, analytical results for the steady state in the limit of weak biasing, $k \ll 1$, can be obtained by following the prescription in Reference 113. Specifically, configurational steady state generated by energy biasing can be generated using an interparticle interaction force field $\tilde{\mathbf{F}}_i$ (46):

$$\tilde{\mathbf{F}}_i = -k/\gamma \nabla_i V_{A-B} + \mathbf{F}_i + \mathcal{O}(k^2).$$
 8.

As a result, the trajectories that consume energy from or release energy into the tracer-bath potential are associated with a physical dynamics in which, at leading order, the A–B interaction strength is simply renormalized by the bias amplitude, *k*. The interactions between A–A and B–B

are unmodified. For a system with purely repulsive interparticle interactions, the effective repulsive interactions between A and B can be further enhanced by tuning k and permitting energy flows into the A–B interactions. Such enhanced repulsions between A and B particles can lead to clustering of like particles consistent with the features observed in a nonequilibrium experiment and/or simulation in which the A particles are driven into the B particles by external fields.

In Figure 4*b*, the effectiveness of this theory is tested (46) by comparing averages generated from biased ensembles [using the cloning algorithm (120, 123–128), in which desired rare realizations are regularly selected and multiplied to efficiently sample the biased ensembles (125)] with those generated from equilibrium dynamics with Equation 8. There is excellent agreement between two-point A–B pair-correlation functions obtained using the two approaches even for intermediate values of $|k| \sim 0.2$. This agreement implies that the result of energy biasing can indeed be anticipated using our theory when the biasing is not strictly in a perturbative regime (46). An analytical solution can also be obtained in a nonperturbative regime, as shown in Reference 46. The nonperturbative solution simply has an extra nonlocal term that enhances clustering.

3.2. Controlling Structure and Phase Transitions Using Energy Dissipation

The model calculation reviewed in the previous section shows how biased energy flows can be used to renormalize interactions. This calculation was inspired by work in References 106 and 108, in which the authors used the large deviation framework to importance-sample trajectories of model active-matter systems according to a measure of the microscopic work done by the active forces, \dot{w} . The rate of work, \dot{w} , can be viewed as an analog of $\varepsilon(t)$ in Equation 7 above, with the caveat that $\varepsilon(t)$ can be defined even for time-symmetric dynamics. In some contexts, it can be shown that the average rate of work, $\langle \dot{w} \rangle$, is proportional to the so-called swim pressure (104).

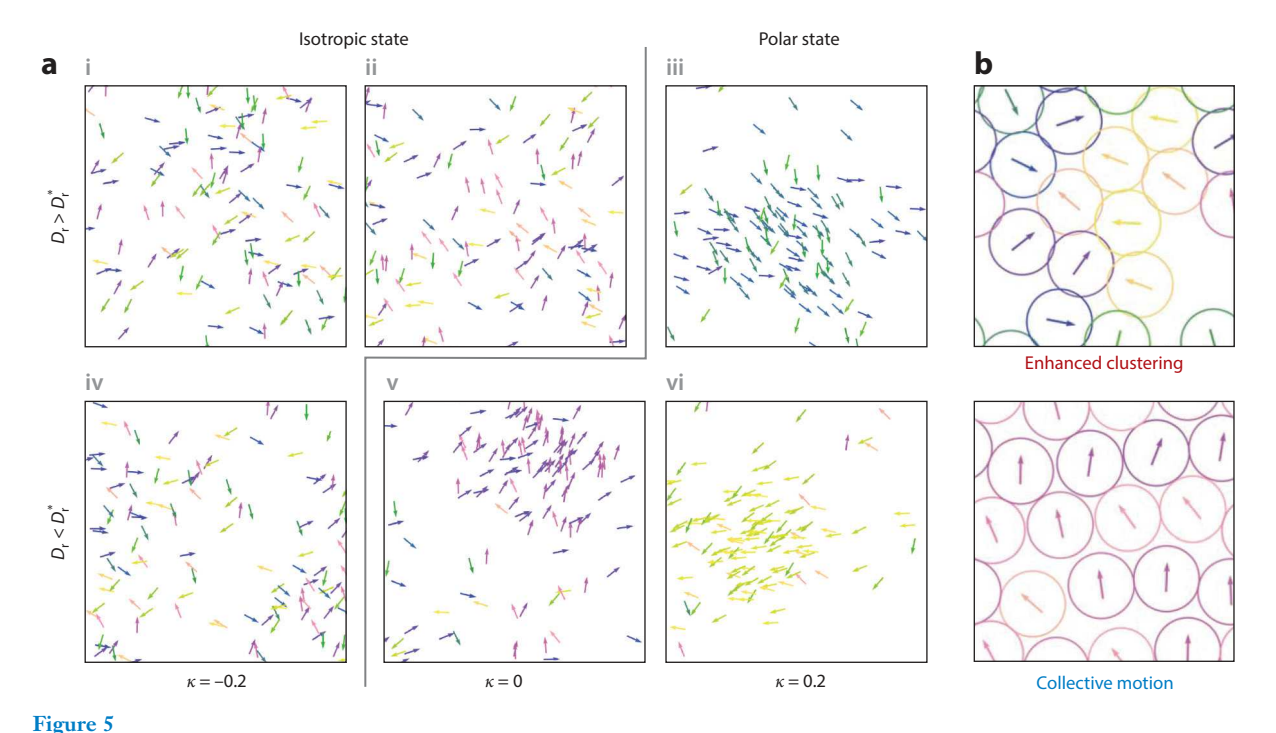
It was demonstrated in References 106 and 108 that commonly observed structural phase transitions in model active-matter systems can be accessed by importance sampling the statistics of \dot{w} . Building on these ideas, in References 46 and 107, it was demonstrated that importance sampling a biased energy-flow rate can also be used to access flocking-like transitions in model nonequilibrium systems (**Figure 5**). Together, these results suggest that the statistics of dissipation can play an important role in controlling various collective phenomena and phase transitions in nonequilibrium systems.

Finally, we end this section by noting that identifying a set of physical dynamical rules that generate an ensemble of trajectories that exactly resemble those generated by importance sampling \dot{w} and other related quantities remains an open question. Nonetheless, it might be possible to develop intuition for physical dynamics that can generate ensembles statistically resembling those generated by importance sampling using an optimal control–like framework (129). We discuss this further in Section 4 below.

4. FUTURE OUTLOOK AND CHALLENGES

4.1. Hydrodynamic Generalizations

In what follows, we envision the future directions for equilibrium growth progress (Sections 4.1–4.5) and organization in driven and active media (Sections 4.6 and 4.7), respectively. In Equation 6 and its various proposed generalizations, we have assumed that the dominant nonequilibrium forces are tied to growth. Our approach does not consider other dissipative effects such as those due to hydrodynamic modes (3) and particle transport, which can be important factors. If the contributions from such considerations are to be considered, Equation 6 needs to be generalized



Energy biasing used to modulate steady-state structures. (a) Configurations obtained from sampling the biased dynamics of a system consisting of aligning self-propelled rods. Simulation details are described in Reference 46. The color-coding describes the orientation of particles. In the unbiased dynamics ($\kappa \sim 0$), we observe isotropic and polar states, respectively, at large noise ($D_r > D_r^*$) and small noise ($D_r < D_r^*$). The dynamical bias leads to renormalizing interactions in a controlled manner (as suggested by Equation 8), which effectively changes the transition threshold, $D_r^* \to D_r^*(1+\kappa)$. As a result, one can stabilize either isotropic or polar states, respectively, simply by tuning the rate of energy flow using κ without modifying the interactions. Panel a adapted from Reference 46. (b) Tuning the rate of work \dot{w} in an active media can be used to access either structurally clustered phases or phases exhibiting collective motion. These results illustrate the ability to trigger or inhibit collective effects in nonequilibrium systems by simply dynamically modulating energy flows or dissipation rates. Panel b adapted from Reference 107.

so that the entropy production rate includes these effects. Following the theoretical framework laid out above, the thermodynamic uncertainty relations can potentially be used to obtain a set of inequalities constraining the fluctuations in various fluxes. Such sets of inequalities can be viewed as generalizations of the classical linear irreversible thermodynamics approach that is commonly used to obtain phenomenological equations of motion in near equilibrium settings (71, 81).

4.2. Thermodynamic Constraints for Time-Dependent Driving

As written, the formalism in Equation 6 cannot be applied to an important class of nonequilibrium self-assembly processes modulated by time-dependent driving. Indeed, time-periodic forcing has been used to create nonequilibrium states with enhanced order in many contexts (4, 130–134). Recent work (85) has shown how the thermodynamic uncertainty relations can be written down even for time-dependent nonequilibrium processes. Adapting these relations to the case of nonequilibrium growth, future work should explore and develop time-dependent versions of Equation 6. If successful, such work has the potential to reveal tradeoffs between energy consumption and organization even in time-dependent nonequilibrium growth processes.

4.3. Modulating Structure and Phase Transformation Behavior of Self-Assembled Colloidal Crystals Using Nonequilibrium Forcing

Building on the results in References 42 and 43, we anticipate that this thermodynamic framework can be used to study the properties of colloidal or nanoscale crystals assembled under nonequilibrium growth conditions. Indeed, experiments and simulations have shown that nonequilibrium forcing can potentially modify crystal structures and phase behavior in such setups (135–137). For example, Reference 137 used computer simulations to study the nonequilibrium phase diagram of a binary A–B mixture. This work showed that the location of the line separating the bodycentered cubic and close-packed phases shifted if the crystals were grown out of equilibrium. The nonequilibrium theoretical framework in Equation 6 can potentially reveal how energy landscapes different from the equilibrium landscapes or, alternatively, how crystals characteristic of interaction energies different than the ones encoded physically can be generated by nonequilibrium forcing (for example, using $\delta\mu$). Such studies can clarify how the equilibrium phase diagram and boundaries can be modified by nonequilibrium forcing (137) (**Figure 2**).

Finally, we anticipate that it might be possible to adapt Equation 6 so that it applies to finite-time thermodynamic processes (82, 83). Then it might be possible to develop predictive thermodynamic frameworks that explain the self-assembly of large complex terminal structures (i.e., finite structures as opposed to the nonterminal assemblies considered above) (138) from patchy nanoparticles (67, 139) and DNA mediated interactions (140).

4.4. Thermodynamic Bounds on Membrane Morphologies Due to Nonequilibrium Activity

Building on the above described applications of Equation 6 to understand nonequilibrium morphologies of model membranes (embedded in two dimensions), future work should explore whether similar relations can be written down for more realistic membrane models that are embedded in three dimensions (**Figure 3b**, **subpanel** *iii*) and to include cases in which detailed balance is broken due to other membrane remodeling events. One important example of this is the binding and unbinding of curvature-preferring proteins, which are often involved in active membrane remodeling processes such as endocytosis and cell fission (94, 141). Nonequilibrium thermodynamic bounds, if derivable in a manner that accounts for the various hydrodynamic flows, can provide intuition for the microscopic energy requirements to drive such organization. Such bounds can provide a general far-from-equilibrium framework for controlling membrane material properties, such as the local surface tension, at the cost of energy consumption.

4.5. Biological Polymerization Reactions

Proofreading mechanisms used during various DNA replication processes provide an illustrative example of the tradeoffs among dissipation, speed, and error or functionality in biology. We anticipate that connections like those in Equation 6 will further elucidate these tradeoffs. Indeed, expressions for entropy production for various model replication processes have already been obtained. Such expressions can be used to extend Equation 6 to study the energy–speed–accuracy tradeoffs in replication and translation processes in biology (75, 79, 80).

Polymerization dynamics also play a very important role in modulating the properties of force transmitting biological agents such as actin and microtubules. Recent experimental and theoretical work has found that the speed of actin polymerization influences the statistics with which various actin bundling proteins bind and bundle the growing actin filaments (142). Adapting Equation 6

to such cases can reveal how the energy dissipation accompanying actin polymerization can in turn support a nonzero reorganization cost, $\langle \epsilon_{\rm diss} \rangle$, for changing the makeup of the actin bundles.

4.6. Modulating Material Properties and Phase Transitions Using Activity

Recent work in References 102 and 143 has shown how the flow of energy through the active nematic material can modify the elastic constants to different degrees and change the mechanics of the material. By adapting relations like Equation 8 so that they can be applied to materials with complex anisotropic interactions, future work should explore the extent to which effective interactions in complex media can be tuned at the cost of energy dissipation. Furthermore, future work should also explore how predictions from Equation 8 (and related identities) can be physically realized using specific nonequilibrium driving protocols. Reference 129 suggests that an optimal control–like framework can be used to develop intuition for nonequilibrium driving protocols that generate ensembles of trajectories closely resembling those generated by importance sampling.

Such progress can help realize the various collective states and regimes predicted in importance-sampled trajectories using physical dynamics. If successful, such work can provide a thermodynamic foundation for understanding how biological materials are able to dynamically modulate their material properties and undergo various complex phase transitions using nonequilibrium activity (19).

4.7. Controlling Complex Self-Assembly Using Energy Dissipation

Results such as those in Equation 8 and References 46, 107, and 144 could be of potential interest for guiding complex self-assembly far from equilibrium (145). For instance, in settings with multiple particle types, it might be possible to renormalize interactions between various sets of particles in a targeted manner by controlling the rates at which energy is dissipated into the interactions. The resultant renormalized interaction-potential landscape might promote spontaneous self-assembly of various structures—at the cost of energy consumption. Progress again requires that results such as those in Equation 8 and References 46 and 107, which are based on a large deviation framework and require the construction of specific biased ensembles, be translated so that they apply to physically realizable driving protocols. If successful, such work could provide a thermodynamic basis for explaining complex nonequilibrium self-assembly, such as that in Reference 101, in which an open Kagome lattice structure was stabilized using nonequilibrium activity.

5. CONCLUSIONS

In this review, we have focused specifically on the extent to which metrics of energy dissipation can be used to constrain the properties of various nonequilibrium systems. Using ideas from stochastic thermodynamics and large deviation theories, we have argued that the statistics of energy dissipation can potentially be used to predict self-assembly properties, correlations, material properties, and phase transition behavior in many nonequilibrium systems. Biology uses nonequilibrium activity to support a variety of novel functional states. We anticipate that the frameworks reviewed here can provide a starting point to address some of the unique phenomenology seen in biophysical systems and potentially replicate them in synthetic materials.

DISCLOSURE STATEMENT

The authors are not aware of any affiliations, memberships, funding, or financial holdings that might be perceived as affecting the objectivity of this review.

ACKNOWLEDGMENTS

We are grateful to Steve Strong and Jordan Horowitz for comments on an earlier version of this manuscript. S.V. and Y.Q. acknowledge support from the University of Chicago Materials Research Science and Engineering Center, which is funded by the National Science Foundation (NSF) under grant no. DMR-1420709. S.V. acknowledges support from the Sloan Foundation and startup funds from the University of Chicago. S.V. acknowledges support from the National Science Foundation under grant no. DMR-1848306. M.N. acknowledges support from the NSF Graduate Research Fellowships Program.

LITERATURE CITED

- 1. Cates ME, Tailleur J. 2015. Annu. Rev. Condens. Matter Phys. 6:219-44
- 2. Battle C, Broedersz CP, Fakhri N, Gever VF, Howard J, et al. 2016. Science 352:604-7
- 3. Driscoll M, Delmotte B, Youssef M, Sacanna S, Donev A, Chaikin P. 2017. Nat. Phys. 13:375-79
- 4. Corté L, Chaikin PM, Gollub JP, Pine DJ. 2008. Nat. Phys. 4:420-24
- 5. Nguyen NHP, Klotsa D, Engel M, Glotzer SC. 2014. Phys. Rev. Lett. 112:075701
- 6. Redner GS, Hagan MF, Baskaran A. 2013. Phys. Rev. Lett. 110:055701
- 7. Marchetti MC, Joanny JF, Ramaswamy S, Liverpool TB, Prost J, et al. 2013. Rev. Mod. Phys. 85:1143-89
- 8. Solon AP, Fily Y, Baskaran A, Cates ME, Kafri Y, et al. 2015. Nat. Phys. 11:673-78
- 9. Mann S. 2009. Nat. Mater. 8:781-92
- 10. Lan G, Sartori P, Neumann S, Sourjik V, Tu Y. 2012. Nat. Phys. 8:422–28
- 11. Lele PP, Hosu BG, Berg HC. 2013. PNAS 110:11839-44
- 12. Tu Y. 2008. PNAS 105:11737-41
- 13. Hopfield JJ. 1974. PNAS 71:4135-39
- 14. Bennett CH. 1979. BioSystems 11:85-91
- 15. Mehta P, Schwab DJ. 2012. PNAS 109:17978-82
- 16. Tu Y, Shimizu TS, Berg HC. 2008. PNAS 105:14855–60
- 17. Wang F, Shi H, He R, Wang R, Zhang R, Yuan J. 2017. Nat. Phys. 13:710-14
- 18. Galkin VE, Orlova A, Egelman EH. 2012. Curr. Biol. 22:R96-101
- 19. Banerjee S, Gardel ML, Schwarz US. 2020. Annu. Rev. Condens. Matter Phys. 11:421-39
- 20. Brugués J, Needleman D. 2014. PNAS 111:18496-500
- 21. Hess H, Ross JL. 2017. Chem. Soc. Rev. 46:5570-87
- 22. Weirich KL, Dasbiswas K, Witten TA, Vaikuntanathan S, Gardel ML. 2019. PNAS 116:11125-30
- 23. Seifert U. 2011. Eur. Phys. J. E 34:26
- 24. Fürthauer S, Lemma B, Foster PJ, Ems-McClung SC, Yu CH, et al. 2019. Nat. Phys. 15:1295-300
- 25. Murrell M, Oakes PW, Lenz M, Gardel ML. 2015. Nat. Rev. Mol. Cell Biol. 16:486-98
- 26. van Esch JH, Klajn R, Otto S. 2017. Chem. Soc. Rev. 46:5474-75
- 27. Grzybowski BA, Fitzner K, Paczesny J, Granick S. 2017. Chem. Soc. Rev. 46:5647-78
- 28. Klajn R, Bishop KJM, Grzybowski BA. 2007. PNAS 104:10305-9
- 29. Lucas LN, van Esch J, Kellogg RM, Feringa BL. 2001. Chem. Commun. 2001:759-60
- 30. de Jong JJD, Hania PR, Pugžlys A, Lucas LN, de Loos M, et al. 2005. Angew. Chem. Int. Ed. 44:2373-76
- 31. Jha PK, Kuzovkov V, Grzybowski BA, Olvera de la Cruz M. 2012. Soft Matter 8:227–34
- 32. Palacci J, Sacanna S, Steinberg AP, Pine DJ, Chaikin PM. 2013. Science 339:936-40
- 33. Schwarz-Linek J, Valeriani C, Cacciuto A, Cates ME, Marenduzzo D, et al. 2012. PNAS 109:4052-57
- 34. Shankar S, Bowick MJ, Marchetti MC. 2017. Phys. Rev. X 7:031039
- 35. Kokot G, Piet D, Whitesides GM, Aranson IS, Snezhko A. 2015. Sci. Rep. 5:9528
- 36. Yan J, Han M, Zhang J, Xu C, Luijten E, Granick S. 2016. Nat. Mater. 15:1095-99
- 37. Minkenberg CB, Florusse L, Eelkema R, Koper GJM, van Esch JH. 2009. J. Am. Chem. Soc. 131:11274–75
- 38. Surrey T, Nédélec F, Leibler S, Karsenti E. 2001. Science 292:1167-71
- 39. Sue ACH, Mannige RV, Deng H, Cao D, Wang C, et al. 2015. PNAS 112:5591–96

- 40. Arango-Restrepo A, Barragán D, Rubi JM. 2018. Phys. Chem. Chem. Phys. 20:4699-707
- 41. Al-Ghoul M, Sultan R. 2001. 7. Phys. Chem. A 105:8053-58
- 42. Nguyen M, Vaikuntanathan S. 2016. PNAS 113:14231-36
- 43. Nguyen M, Vaikuntanathan S. 2018. Phys. Rev. E. arXiv:1803.04368 [cond-mat.soft]
- 44. del Junco C, Tociu L, Vaikuntanathan S. 2018. PNAS 115:3569-74
- 45. del Junco C, Vaikuntanathan S. 2019. *J. Chem. Phys.* 150:094708
- 46. Tociu L, Fodor E, Nemoto T, Vaikuntanathan S. 2019. Phys. Rev. X 9:041026
- 47. Murugan A, Vaikuntanathan S. 2017. Nat. Commun. 8:13881
- 48. Dasbiswas K, Mandadapu KK, Vaikuntanathan S. 2018. PNAS 115:E9031-40
- 49. Fleming GR, Ratner MA. 2008. Phys. Today 61:28-33
- 50. Whitesides GM, Grzybowski B. 2002. Science 295:2418-21
- 51. Seifert U. 2011. Phys. Rev. Lett. 106:020601
- 52. Esposito M, Van den Broeck C. 2010. Phys. Rev. E 82:011143
- 53. Seifert U. 2012. Rep. Prog. Phys. 75:126001
- 54. Fodor É, Nardini C, Cates ME, Tailleur J, Visco P, van Wijland F. 2016. Phys. Rev. Lett. 117:38103
- 55. Whitelam S, Schulman R, Hedges L. 2012. Phys. Rev. Lett. 109:265506
- 56. Whitelam S, Hedges LO, Schmit JD. 2014. Phys. Rev. Lett. 112:155504
- 57. Barato AC, Seifert U. 2015. Phys. Rev. Lett. 114:158101
- 58. Gingrich TR, Horowitz JM, Perunov N, England JL. 2016. Phys. Rev. Lett. 116:120601
- 59. Touchette H. 2009. Phys. Rep. 478:1-69
- 60. Ke Y, Ong LL, Shih WM, Yin P. 2012. Science 338:1177-83
- 61. Jones MR, Seeman NC, Mirkin CA. 2015. Science 347:1260901
- 62. Reinhardt A, Frenkel D. 2014. Phys. Rev. Lett. 112:238103
- 63. Hedges LO, Mannige RV, Whitelam S. 2014. Soft Matter 10:6404–16
- 64. Glotzer SC. 2012. Nature 481:450-52
- 65. Mao X, Chen Q, Granick S. 2013. Nat. Mater. 12:217–22
- 66. Miller WL, Cacciuto A. 2009. Phys. Rev. E 80:021404
- 67. Glotzer SC, Solomon MJ. 2007. Nat. Mater. 6:557–62
- 68. Whitelam S. 2010. J. Chem. Phys. 132:194901
- 69. Hormoz S, Brenner MP. 2011. PNAS 108:5193-98
- 70. Jarzynski C. 2011. Annu. Rev. Condens. Matter Phys. 2:329-51
- 71. Doi M. 2011. 7. Phys.: Condens. Matter 23:284118
- 72. Falzone TT, Lenz M, Kovar DR, Gardel ML. 2012. Nat. Commun. 3:861
- 73. Ruiz-Herrero T, Fai TG, Mahadevan L. 2019. Phys. Rev. Lett. 123:038102
- 74. Lenz M, Witten TA. 2017. Nat. Phys. 13:1100-4
- 75. Andrieux D, Gaspard P. 2008. PNAS 105:9516-21
- 76. Schnakenberg J. 1976. Rev. Mod. Phys. 48:571-85
- 77. Andrieux D, Gaspard P. 2007. J. Stat. Phys. 127:107-31
- 78. Gaspard P, Andrieux D. 2014. 7. Chem. Phys. 141:044908
- 79. Sartori P, Pigolotti S. 2015. Phys. Rev. X 5:041039
- 80. Poulton JM, ten Wolde PR, Ouldridge TE. 2019. PNAS 116:1946-51
- 81. de Groot SR, Mazur PP. 1984. Non-Equilibrium Thermodynamics. New York: Dover
- 82. Pietzonka P, Ritort F, Seifert U. 2017. Phys. Rev. E 96:012101
- 83. Horowitz JM, Gingrich TR. 2017. Phys. Rev. E 96:020103
- 84. Koyuk T, Seifert U. 2019. Phys. Rev. Lett. 122:230601
- 85. Barato AC, Chetrite R, Faggionato A, Gabrielli D. 2018. N. 7. Phys. 20:103023
- 86. Gingrich TR, Horowitz JM. 2017. Phys. Rev. Lett. 119:170601
- 87. McMahon HT, Gallop JL. 2005. Nature 438:590–96
- 88. Gowrishankar K, Ghosh S, Saha S, Rumamol C, Mayor S, Rao M. 2012. Cell 149:1353-67
- 89. Stachowiak JC, Schmid EM, Ryan CJ, Ann HS, Sasaki DY, et al. 2012. Nat. Cell Biol. 14:944-49
- 90. Chen Z, Atefi E, Baumgart T. 2016. Biophys. 7. 111:1823–26

- 91. Turlier H, Fedosov DA, Audoly B, Auth T, Gov NS, et al. 2016. Nat. Phys. 12:513–20
- 92. Solon J, Pécréaux J, Girard P, Fauré MC, Prost J, Bassereau P. 2006. Phys. Rev. Lett. 97:3-6
- 93. Dervaux J, Noireaux V, Libchaber AJ. 2017. Eur. Phys. 7. Plus 132:284
- 94. Rao M, Sarasij RC. 2001. Phys. Rev. Lett. 87:128101
- 95. Fily Y, Marchetti MC. 2012. Phys. Rev. Lett. 108:235702
- 96. Mallory SA, Cacciuto A. 2016. Phys. Rev. E 94:022607
- 97. Mallory SA, Valeriani C, Cacciuto A. 2018. Annu. Rev. Phys. Chem. 69:59-79
- 98. Han M, Yan J, Granick S, Luijten E. 2017. PNAS 114:7513-18
- 99. Yan J, Bae SC, Granick S. 2015. Soft Matter 11:147-53
- 100. Yan J, Bloom M, Bae SC, Luijten E, Granick S. 2012. Nature 491:578-81
- 101. Mallory SA, Cacciuto A. 2019. 7. Am. Chem. Soc. 141:2500-7
- 102. Joshi A, Putzig E, Baskaran A, Hagan MF. 2019. Soft Matter 15:94-101
- 103. Solon AP, Stenhammar J, Wittkowski R, Kardar M, Kafri Y, et al. 2015. Phys. Rev. Lett. 114:198301
- 104. Takatori SC, Brady JF. 2015. Phys. Rev. E 91:032117
- 105. Solon AP, Stenhammar J, Cates ME, Kafri Y, Tailleur J. 2018. N. 7. Phys. 20:075001
- 106. Cagnetta F, Corberi F, Gonnella G, Suma A. 2017. Phys. Rev. Lett. 119:158002
- 107. Fodor É, Nemoto T, Vaikuntanathan S. 2020. N. 7. Phys. 22:013052
- 108. Nemoto T, Fodor E, Cates ME, Jack RL, Tailleur J. 2019. Phys. Rev. E 99:022605
- Garrahan JP, Jack RL, Lecomte V, Pitard E, van Duijvendijk K, van Wijland F. 2007. Phys. Rev. Lett. 98:195702
- 110. Hedges LO, Jack RL, Garrahan JP, Chandler D. 2009. Science 323:1309-13
- 111. Pitard E, Lecomte V, van Wijland F. 2011. Europhys. Lett. 96:56002
- 112. Speck T, Engel A, Seifert U. 2012. J. Stat. Mech.: Theory Exp. 2012:P12001
- 113. Chetrite R, Touchette H. 2013. Phys. Rev. Lett. 111:120601
- 114. Jack RL, Sollich P. 2010. Prog. Theor. Phys. Suppl. 184:304-17
- Gardiner CW. 1985. Handbook of Stochastic Methods for Physics, Chemistry, and the Natural Sciences. Berlin/Heidelberg: Springer. 2nd ed.
- 116. Speck T, Malins A, Royall CP. 2012. Phys. Rev. Lett. 109:195703
- 117. Bodineau T, Lecomte V, Toninelli C. 2012. 7. Stat. Phys. 147:1–17
- 118. Limmer DT, Chandler D. 2014. PNAS 111:9413-18
- 119. Nemoto T, Hidalgo EG, Lecomte V. 2017. Phys. Rev. E 95:012102
- 120. Tailleur J, Kurchan J. 2007. Nat. Phys. 3:203-7
- 121. Laffargue T, Thu-Lam KDN, Kurchan J, Tailleur J. 2013. J. Phys. A: Math. Theor. 46:254002
- 122. Whitelam S, Klymko K, Mandal D. 2018. J. Chem. Phys. 148:154902
- 123. Giardinà C, Kurchan J, Peliti L. 2006. Phys. Rev. Lett. 96:120603
- 124. Hurtado PI, Garrido PL. 2009. Phys. Rev. Lett. 102:250601
- 125. Nemoto T, Bouchet F, Jack RL, Lecomte V. 2016. Phys. Rev. E 93:062123
- 126. Ray U, Chan GKL, Limmer DT. 2018. Phys. Rev. Lett. 120:210602
- 127. Klymko K, Geissler PL, Garrahan JP, Whitelam S. 2018. Phys. Rev. E 97:032123
- 128. Brewer T, Clark SR, Bradford R, Jack RL. 2018. J. Stat. Mech.: Theory Exp. 2018:053204
- 129. Jack RL. 2020. Eur. Phys. 7. B 93:74
- 130. Lumsdon SO, Kaler EW, Velev OD. 2004. *Langmuir* 20:2108–16
- 131. Singh JP, Lele PP, Nettesheim F, Wagner NJ, Furst EM. 2009. Phys. Rev. E 79:050401
- 132. Tagliazucchi M, Weiss EA, Szleifer I. 2014. PNAS 111:9751-56
- 133. Helbing D, Farkas IJ, Vicsek T. 2000. Phys. Rev. Lett. 84:1240-43
- 134. Stanley HE. 2000. Nature 404:718-19
- 135. Rogers WB, Shih WM, Manoharan VN. 2016. Nat. Rev. Mater. 1:16008
- 136. Zeravcic Z, Manoharan VN, Brenner MP. 2017. Rev. Mod. Phys. 89:031001
- 137. Scarlett RT, Ung MT, Crocker JC, Sinno T. 2011. Soft Matter 7:1912–25
- 138. Tkachenko AV. 2011. Phys. Rev. Lett. 106:255501
- 139. Zhang Z, Glotzer SC. 2004. Nano Lett. 4:1407-13
- 140. Jacobs WM, Reinhardt A, Frenkel D. 2015. PNAS 112:6313-18

- 141. Ramakrishnan N, Ipsen JH, Rao M, Kumar PBS. 2015. Soft Matter 11:2387-93
- 142. Freedman SL, Suarez C, Winkelman JD, Kovar DR, Voth GA, et al. 2019. PNAS 116:16192-97
- 143. Zhang J, Luijten E, Grzybowski BA, Granick S. 2017. Chem. Soc. Rev. 46:5551-69
- 144. GrandPre T, Klymko K, Mandadapu KK, Limmer DT. 2020. arXiv:2007.12149 [cond-mat.stat-mech]
- 145. Bisker G, England JL. 2018. PNAS 115:E10531-38



Contents

Annual Review of Condensed Matter Physics

Volume 12, 2021

Have I Really Been a Condensed Matter Theorist? I'm Not Sure, but Does It Matter? Edouard Brézin	1
A Career in Physics Bertrand I. Halperin	15
Mechanical Frequency Tuning by Sensory Hair Cells, the Receptors and Amplifiers of the Inner Ear Pascal Martin and A.J. Hudspeth	29
On the Role of Competing Interactions in Charged Colloids with Short-Range Attraction José Ruiz-Franco and Emanuela Zaccarelli	51
The Fracture of Highly Deformable Soft Materials: A Tale of Two Length Scales Rong Long, Chung-Yuen Hui, Jian Ping Gong, and Eran Bouchbinder	71
Modeling Grain Boundaries in Polycrystalline Halide Perovskite Solar Cells Fi-Sang Park and Aron Walsh	95
Creep Motion of Elastic Interfaces Driven in a Disordered Landscape Ezequiel E. Ferrero, Laura Foini, Thierry Giamarchi, Alejandro B. Kolton, and Alberto Rosso	111
Stem Cell Populations as Self-Renewing Many-Particle Systems David J. Jörg, Yu Kitadate, Shosei Yoshida, and Benjamin D. Simons	135
Polyelectrolyte Complex Coacervates: Recent Developments and New Frontiers Artem M. Rumyantsev, Nicholas E. Jackson, and Juan J. de Pablo	155
Enzymes as Active Matter Subhadip Ghosh, Ambika Somasundar, and Ayusman Sen	177
Symmetry Breaking and Nonlinear Electric Transport in van der Waals Nanostructures Toshiya Ideue and Yoshihiro Iwasa	201

Band Representations and Topological Quantum Chemistry Jennifer Cano and Barry Bradlyn	225
Topology and Symmetry of Quantum Materials via Nonlinear Optical	
Responses	
J. Orenstein, J.E. Moore, T. Morimoto, D.H. Torchinsky, J.W. Harter,	
and D. Hsieh	247
Organization and Self-Assembly Away from Equilibrium:	
Toward Thermodynamic Design Principles	
Michael Nguyen, Yuqing Qiu, and Suriyanarayanan Vaikuntanathan	273

Errata

An online log of corrections to *Annual Review of Condensed Matter Physics* articles may be found at http://www.annualreviews.org/errata/conmatphys